Physicochemical Characterization of Chromium Oxides Immobilized in Mesoporous MeMCM-41 (Me = Al, Ti, and Zr) Molecular Sieves

Zhidong Zhu,[†] Martin Hartmann,[‡] Estelle M. Maes,[†] Roman S. Czernuszewicz,[†] and Larry Kevan*[,†]

Department of Chemistry, University of Houston, Houston, Texas 77204-5641, and Department of Chemistry, Chemical Technology, University of Kaiserslautern, D-67763 Kaiserslautern, Germany

Received: December 9, 1999; In Final Form: February 7, 2000

A series of mesoporous siliceous MCM-41 (SiMCM-41) molecular sieves with silicon partially substituted by Al, Ti, and Zr were synthesized hydrothermally. A combination of electron spin resonance (ESR), diffuse reflectance UV−vis spectroscopy (UV−vis), Raman spectroscopy, and temperature-programmed reduction (TPR) was used successfully to characterize the chemical environment of chromium in Cr/MeMCM-41 (Me = Al, Ti, and Zr). UV−vis, ESR, and Raman spectroscopy show that Cr_2O_3 is present in SiMCM-41, ZrMCM-41, and AlMCM-41. With increasing Al content in AlMCM-41, the amount of Cr_2O_3 increases, which contrasts with $Cr/SiO_2{\cdot}Al_2O_3$. Cr_2O_3 is reduced in Cr/TiMCM-41 with a Si/Ti ratio of less than 25 compared to higher ratios. The results reveal a strong interaction between chromium and surface titanium centers, which immobilizes the chromium species and reduces the formation of Cr_2O_3. UV−vis and Raman spectra show that Cr/MeMCM-41 materials are dominated by dichromate. The overall intensity of Cr(V) increases in the order AlMCM-41 < SiMCM-41 < TiMCM-41 < ZrMCM-41. The intensity of Cr_2O_3 increases in the order of TiMCM-41 < ZrMCM-41 < SiMCM-41 < AlMCM-41. These results show that Ti and Zr stabilize Cr(V) and Cr(VI) compared to Al and Si.

Introduction

Supported chromium oxides consisting of a surface monolayer dispersed on a high surface area oxide support such as TiO_2, ZrO_2, Al_2O_3, and SiO_2 have been used as commercial catalysts for polymerization, dehydrogenation, and selective catalytic reduction (SCR) of NO_x.[1] To control the molecular weight of high-density polyethylene polymer, Ti and Al oxides are often incorporated into a silica support to form $Cr/TiO_2/SiO_2$ and $Cr/Al_2O_3/SiO_2$ catalysts, which produce a polymer with a lower average molecular weight and a broader molecular weight distribution.[2−5] The promotional effect of titania is thought to be due to the formation of Cr−O−Ti−O−Si bridging bonds.[2] In addition, chromia alone appears to be practically inactive as a catalyst for ethylene polymerization. The appearance of crystalline and amorphous Cr_2O_3 on a support surface is usually regarded as symptomatic of catalyst deactivation.[6] In the past decade, considerable effort has been devoted to understanding the structure of these catalysts and their catalytic effect on reactivity and selectivity.[7,8] Studies of chromium on these supports have been carried out by infrared spectroscopy (IR), X-ray photoelectron spectroscopy (XPS), Raman spectroscopy, diffuse reflectance UV−vis spectroscopy (UV−vis), electron spin resonance (ESR), and temperature-programmed reduction (TPR).[1] For Cr/SiO_2, it is found that monochromate on Cab-O-Sil material changes to a mixture of monochromate and dichromate (polychromate) on sol−gel material. At higher loadings (>0.1 wt %), dichromate (polychromate) species are always the dominant species. For Cr/Al_2O_3, with Cr typically lower than 1 wt %, monochromate is the dominant species. At higher loadings, polychromates are the dominant species.[1] Anchored chromium oxide species on titania and zirconia are also predominately present as polychromate species.[1] In addition to chromate, Cr(V) ions and Cr_2O_3 clusters are also formed and are easily detectable by ESR.[1] The ratio of surface monochromate to polychromate species and the amounts of Cr(V) and Cr_2O_3 are dependent on support, loading, and sample treatment.

MCM-41 possesses uniform channels varying from about 15 to 100 Å with a large surface area up to 1000 m^2/g.[9a] This makes it a suitable support for transition metal oxides. To our knowledge, chromium supported on MCM-41 with framework aluminum (Cr/AlMCM-41), titanium (Cr/TiMCM-41), zirconium (Cr/ZrMCM-41) and silicon (Cr/SiMCM-41) have not been studied except for a recent communication.[8b] (Al, Ti, Zr) MCM-41 were synthesized and used as supports to prepare Cr/MeMCM-41 by incipient wetness impregnation. ESR, UV−vis, Raman spectroscopies, and TPR are employed to study the chemical environment of chromium in these materials. The results show that chromium(VI) and chromium(V) are highly dispersed in TiMCM-41, whereas Cr_2O_3 appears in (Zr, Al, Si)MCM-41.

Experimental Section

Sample Synthesis and Treatment. MeMCM-41 (Me = Ti and Zr) and SiMCM-41 were synthesized following a modified method for siliceous MCM-41. A typical synthesis procedure is as follows. Ten grams of a 35 wt % solution of tetraethylammonium hydroxide (TEAOH) is combined with 6.2 g of cetyltrimethylammonium bromide (CTAB) dispersed in 49 g of water while stirring and heating at 50 °C for 0.5 h; then, 6 g of silica is added, followed by stirring for 2 h. An amount of titanium isopropoxide $Ti[OCH(CH_3)_2]_4$ or zirconium isopropoxide $Zr[OCH(CH_3)_2]_4$ for the desired Si/Me(Me = Ti and

* To whom correspondence should be addressed.
[†] University of Houston.
[‡] University of Kaiserslauten.

10.1021/jp994335i CCC: $19.00
Published on Web 04/26/2000

Zr) ratio is dissolved in 5 g of water and then slowly added to the silica solution with stirring. The pH of the mixture is adjusted to 11.5 by addition of dilute sulfuric acid. Finally, the gel mixture is transferred into a Teflon-lined autoclave and heated at 150 °C for 2 days. The molar composition of the final gel mixture was 1.0 SiO_2:0.17 CTAB:xMO_2:0.24 TEAOH: 30 H_2O, with $x = 0$ for MCM-41, $x = 0.017-0.10$ for TiMCM-41, and $x = 0.04$ for ZrMCM-41. The solid products were recovered by filtration, washed with deionized water, and dried in air. These samples are designated as MeMCM-41-(x), where x is the Si/Me ratio in the gel, or SiMCM-41 for purely siliceous MCM-41. AlMCM-41 synthesis was performed according to the literature.[9b] As-synthesized samples were calcined by raising the temperature slowly to 540 °C in N_2 and then keeping the sample at this temperature for 15 h in air for removal of CTAB.

Chromium oxide supported catalysts were prepared by the incipient wetness technique with aqueous CrO_3. Various amounts of a CrO_3 solution were mixed with the support under continuous stirring for 2 h. Chromium-impregnated samples were dried at 100 °C overnight. Thereafter, the samples were calcined in flowing air while the temperature was raised from room temperature to 540 °C over a period of 3 h and were kept at 540 °C for 5 h. The samples were then cooled in ambient air and became hydrated. The loading of Cr was 2 wt % for all supports, which is similar to the 1 wt % used for many commercial catalysts.

Measurements. Powder XRD patterns of the calcined products were obtained on a Philips 1840 diffractometer with Cu−Kα radiation (40 kV, 25 mA) at a 0.01° step size and 1s step time over the range $1.2° < 2\theta < 10°$. The samples were prepared as thin layers on aluminum slides.

The diffuse reflectance UV−vis spectra were measured with a Perkin-Elmer 330 spectrophotometer equipped with a 60-mm Hitachi integrating sphere accessory. Powder samples were loaded into a quartz cell with Suprasil windows, and spectra were collected in the 200−800-nm wavelength range against a SiMCM-41 standard.

X-band ESR spectra were recorded in sealed Suprasil quartz tubes at 77 and 350 K with a Bruker ESP 300 ESR spectrometer. The program MAGRES[10] was used to simulate the ESR spectra by choosing suitable g values and line widths to fit the experimental spectra.

The TPR experiments were carried out in a gas flow system equipped with a gradientless microreactor, using an Altamira AMI 1 instrument. The 10 vol % H_2/Ar mixture was fed to a catalyst sample. To collect the water evolved during the reduction, which has been found to affect the position of the TPR peaks for some alumina-supported oxides, a drying tube containing molecular sieve 4A was inserted after the reactor. Approximately 40 mg of sample was activated in flowing Ar at 400 °C for 1 h. For TPR measurements, the temperature was raised from 30 °C to 600 °C at 3 °C/min. The hydrogen consumption was analyzed with a thermal conductivity detector.

Raman spectra were obtained at room temperature using excitation lines from Coherent 90−6 Ar^+ (514.5 nm) and K-2 Kr^+ (406.7 nm) ion lasers, collecting backscattered photons directly from the surface of spinning (∼2000 rpm) solid samples in 7-mm diameter pressed pellets. Conventional scanning Raman instrumentation equipped with a Spex 1403 double monochromator, with a pair of gratings with 1800 grooves/mm, and a cooled Hamamatsu 928 photomultiplier detector was used to record the spectra under the control of a Spex DM3000 microcomputer system, as described elsewhere.[11] Multiple scans (2−5) were averaged to improve the signal-to-noise ratio.

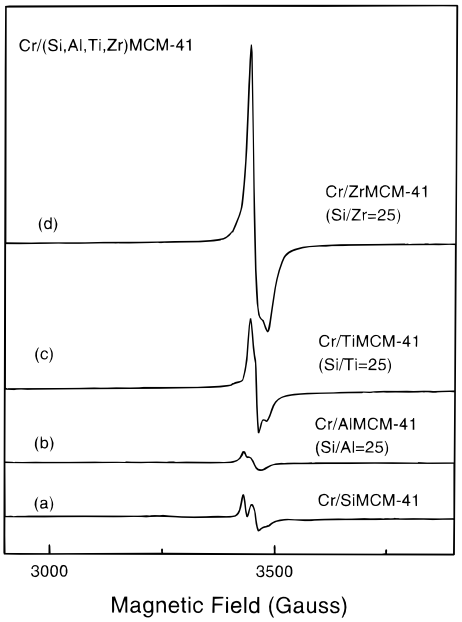

Figure 1. ESR spectra at 77 K of Cr/MeMCM-41 (Me = Al, Ti, and Zr) with Si/Me = 25 and Cr/SiMCM-41: (a) Cr/SiMCM-41, (b) Si/Al = 25, (c) Si/Ti = 25, and (d) Si/Zr = 25.

Typically, each scan was obtained with 30-mW laser power and a slit width of 5 cm^{-1} for hydrated Cr/AlMCM-41 (514.5 nm) and 20-mW laser power and a slit width of 8 cm^{-1} for hydrated Cr/TiMCM-41 (406.7 nm). Since the Cr/TiMCM-41 samples have weak fluorescence at 406.7 nm and stronger fluorescence at 514.5 nm, they are measured at 406.7 nm. The spectrometer was advanced in 1-cm^{-1} increments, and integration times were 1 s per data point. Slowly sloping baselines for some of the samples were subtracted from digitally collected spectra by using LabCalc software (Galactic Industries) on a 486-DX 66 MHz PC microcomputer.

Results

ESR Spectra. There are several reports on ESR investigations of chromium species on the surfaces of SiO_2, Al_2O_3, TiO_2, and ZrO_2.[12−16] Three signals have been found in the ESR spectra of Cr-supported catalysts, which are denoted as γ, β, and δ. The γ-signal is a sharp axially symmetric signal around $g = 1.9$, attributed to isolated, mononuclear Cr(V) species. The β-signal is ascribed to Cr_2O_3-like clusters. The δ-signal is usually assigned to magnetically isolated or dispersed Cr(III) species. The nature of these signals is support-, loading- and treatment-dependent.

ESR of Cr(V): γ Signal. Framework Metal Ions. Figure 1 shows the influence of different framework metal ions on the 77 K ESR spectra of Cr(V). Table 1 reports the ESR parameters obtained by simulation of the experimental spectra. For comparison, the ESR parameters of Cr(V) on oxide supports are also included. The signals are usually interpreted as due to a tetrahedral CrO_4^{3-} species with $g_\perp = 1.985$ and $g_\parallel = 1.906$ and a square pyramidal species with $g_\perp = 1.973-1.976$ and $g_\parallel = 1.955-1.957$. Similar to Cr(V)/$SiO_2$, these two signals are also observed in SiMCM-41. On Cr/AlMCM-41, the spectrum is best fit by overlap of two isotropic species with $g = 1.980$ and $g = 1.973$. On Cr(V)/Al_2O_3, a signal with $g_{av} = 1.971$ is observed and assigned to square-pyramidal Cr(V). The line width increases from SiMCM-41 to AlMCM-41 due to interaction of the unpaired electron of Cr(V) with the ^{27}Al nuclei ($I = 5/2$), which is also observed between silica and alumina. On Cr/

TABLE 1: ESR Parameters of Cr(V) Species on Cr/(Zr, Al, Si, Ti)MCM-41, ZrO_2, Al_2O_3, SiO_2 and TiO_2

sample	species[a]	$g_\perp$	$g_\parallel$	ref
Cr/ZrO_2	Cr(sp)	1.977	1.953	11, 14, 15
Cr/ZrMCM-41	Cr(sp)	1.976	1.955	this work
Cr/TiO_2	Cr(sp)	1.977	1.945	11, 13
Cr/TiMCM-41	Cr(sp)	1.976	1.957	this work
Cr/Al_2O_3	Cr	$g_{av} = 1.971$		11, 12
Cr/AlMCM-41	Cr(O_h)	$g = 1.980$		this work
	Cr(O_h)	$g = 1.973$		
Cr/SiO_2	Cr(T_d)	1.975−1.968	1.895	11, 12
	Cr(sp)	1.975	1.950	
Cr/SiMCM-41	Cr(T_d)	1.985	1.906	this work
	Cr(sp)	1.973	1.957	

[a] sp, square pyramidal: T_d, tetrahedral: O_h, octahedral.

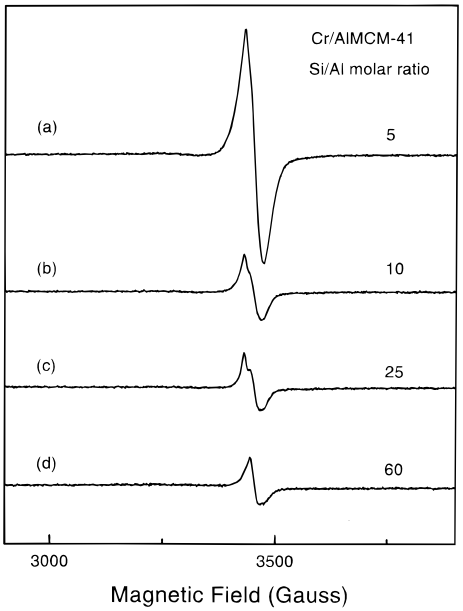

Figure 2. ESR spectra at 77 K of Cr/AlMCM-41 with various Si/Al ratios: (a) Si/Al = 5, (b) Si/Al = 10, (c) Si/Al = 25, and (d) Si/Al = 60.

TiMCM-41 and Cr/ZrMCM-41, only square-pyramidal Cr(V) is observed, similar to Cr(V) on ZrO_2 and TiO_2. The overall ESR intensity determined by double integration of Cr(V) increases in the order Cr/AlMCM-41 < Cr/SiMCM-41 < Cr/TiMCM-41 < Cr/ZrMCM-41.

Framework Si/Al and Si/Ti Ratios. Figures 2 and 3 show 77 K ESR spectra of Cr(V) in Cr/AlMCM-41 and Cr/TiMCM-41, with various amounts of framework Al and Ti. The line width and intensity increase with decreasing Si/Al and Si/Ti ratios. On Cr/AlMCM-41 from Si/Al = 60 to 5, the intensity ratio of the $g = 1.980$ signal to the $g = 1.973$ signal decreases. The signal with $g_\perp = 1.976$ and $g_\parallel = 1.957$ predominates in Cr/TiMCM-41 with different Si/Ti ratios.

ESR of Cr(III): β Signal. Framework Metal Ions. Figure 4 shows the effect of different framework metal ions on the 350 K ESR spectra of Cr(III). The ESR spectra consist of a symmetrical Lorentzian line at $g = 1.98$ with a peak-to-peak line width at 500 G, which disappear abruptly below 350 K and hence shows typical behavior of ESR spectra from α-Cr_2O_3 with a Neel temperature of 308 K. The signal is therefore assigned to α-Cr_2O_3 on the surface of MCM-41. It is remarkable that the β signal is significantly reduced for Cr/TiMCM-41 with Si/Ti = 25. This is supported by Raman results (see below). The intensity of this β signal increases in the order of Cr/ZrMCM-41 < Cr/SiMCM-41 < Cr/AlMCM-41.

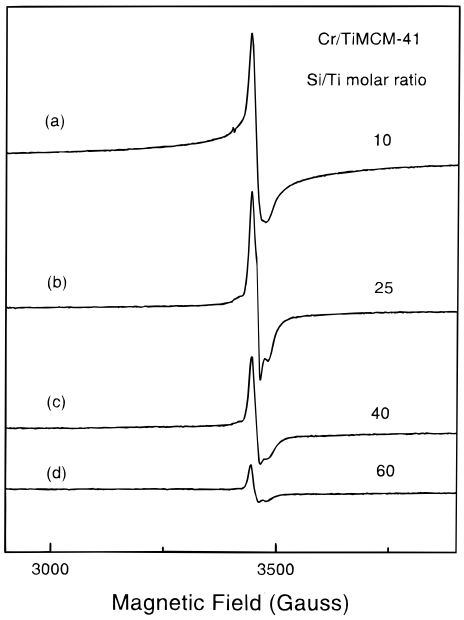

Figure 3. ESR spectra at 77 K of Cr/TiMCM-41 with various Si/Ti ratios: (a) Si/Ti = 10, (b) Si/Al = 25, (c) Si/Al = 40, and (d) Si/Al = 60.

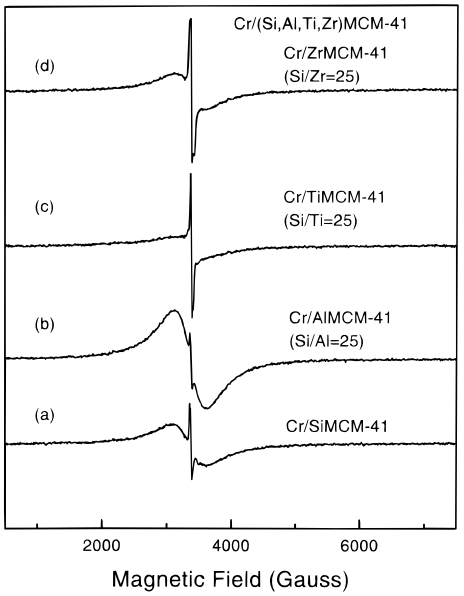

Figure 4. ESR spectra at 350 K of Cr/MeMCM-41 (Me = Al, Ti, and Zr) with Si/Me = 25 and Cr/SiMCM-41: (a) Cr/SiMCM-41, (b) Si/Al = 25, (c) Si/Ti = 25, and (d) Si/Zr = 25.

Framework Si/Al and Si/Ti Ratios. Figures 5 and 6 show 350 K ESR spectra of Cr(III) in Cr/AlMCM-41 and Cr/TiMCM-41 with variable amounts of framework Al and Ti. The line width of the β signal remains the same, whereas the intensity increases with a decreasing Si/Al ratio. This indicates that the amount of Cr_2O_3 increases with increasing framework aluminum content in Cr/AlMCM-41. For Cr/TiMCM-41, the opposite trend is observed. At a higher Si/Ti ratio, a β signal is observed that is reduced at Si/Ti = 25. For Si/Ti = 60, a broad signal at $g = 3$ is observed, which is tentatively attributed to Cr(III) interacting with Ti(III), that is, Cr(III)-O−Ti(III), which also was observed on Cr/TiO_2 with 10 wt % chromium.[14]

ESR of Cr(III): δ Signal. For Cr/AlMCM-41 with Si/Al = 5, a signal at $g = 5$ is observed (Figure 5). The intensity increases with decreasing temperature, as expected from the Curie law. The relative intensity of the δ signal to the β signal

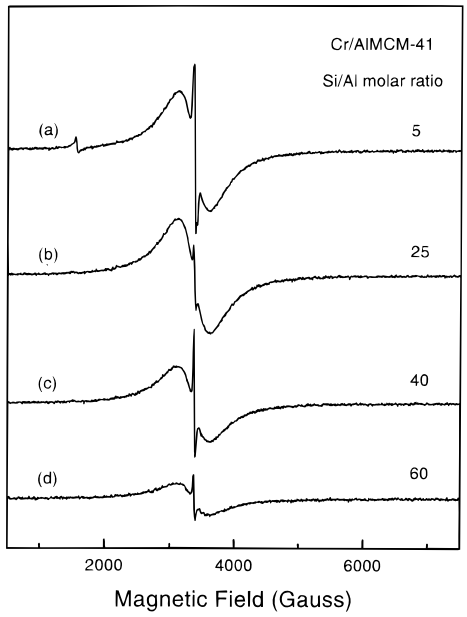

Figure 5. ESR spectra at 350 K of Cr/AlMCM-41 with various Si/Al ratios: (a) Si/Al = 5, (b) Si/Al = 25, (c) Si/Al = 40, and (d) Si/Al = 60.

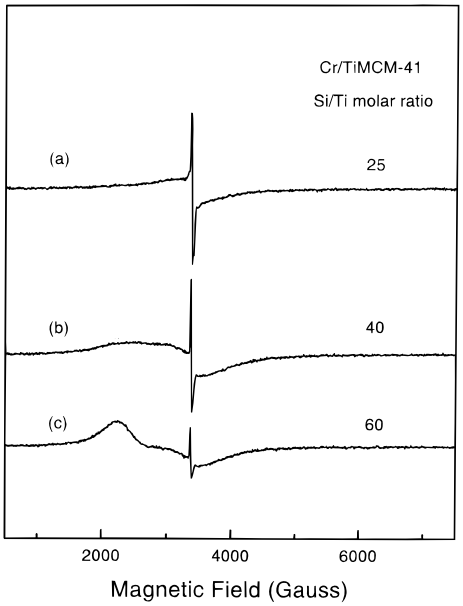

Figure 6. ESR spectra at 350 K of Cr/TiMCM-41 with various Si/Ti ratios: (a) Si/Ti = 25, (b) Si/Ti = 40, and (c) Si/Ti = 60.

is less than 2%. The signal is not observed for Cr/ZrMCM-41 and Cr/TiMCM-41, but it is observed for Cr/TiO_2 and Cr/ZrO_2. It is also absent for SiO_2 and SiMCM-41. This low-field absorption is designated as a δ signal in the literature and is assigned to isolated Cr(III) ions in relatively strong axial crystal fields with distortions of lower symmetry and zero-field splitting of $D = 0.5$ cm^{-1}.[14] This suggests that isolated Cr(III) ions are stabilized in CrAlMCM-41.

UV−Vis Spectra. *Framework Si/Al Ratio.* UV−vis spectroscopy has been extensively used to characterize the nature and coordination of Cr on oxide supports.[17−22] The diffuse reflectance UV−vis spectra of supported chromium oxide catalysts are composed of charge transfer and d−d transitions of chromate, dichromate, and Cr(III), the band maxima of which are given in Table 1 of ref 17. Figure 7 shows the UV−vis spectra of Cr/AlMCM-41 with various Si/Al ratios. All these spectra

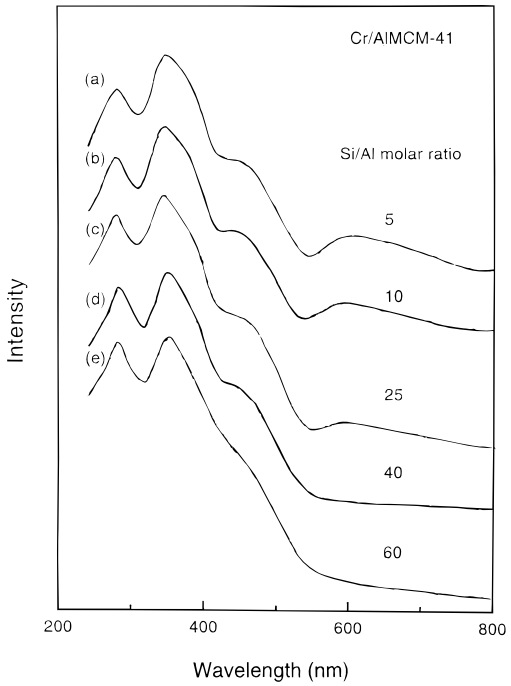

Figure 7. Diffuse reflectance UV−vis spectra of Cr/AlMCM-41 with various Si/Al ratios: (a) Si/Al = 5, (b) Si/Al = 10, (c) Si/Al = 25, (d) Si/Al = 40, and (e) Si/Al = 60.

are dominated by two intense O → Cr(VI) charge-transfer bands of dichromate around 280 and 350 nm. The concentration of chromate (main absorptions at 275 and 370 nm) in Cr/AlMCM-41 is negligible. A shoulder around 445 nm and a broad band around 600 nm both increase with increasing aluminum content. These two bands are assigned to $^4A_{2g} \rightarrow {}^4T_{2g}$ and $^4A_{2g} \rightarrow {}^4T_{1g}$ transitions of Cr(III) in Cr_2O_3, respectively. This conclusion is consistent with the ESR results that show an increase of Cr_2O_3 with increasing Al content in Cr/AlMCM-41. This finding is also supported by Raman results, as shown below.

Framework Si/Ti Ratio. UV−vis spectroscopy has been extensively used to characterize the nature and coordination of Ti(IV) ions in titanium-substituted molecular sieves. A broad band centered at 265 nm is observed in all samples, the intensity of which increases monotonically with increasing titanium content (not shown). Such a band can be assigned to a low-energy charge-transfer transition between tetrahedral oxygen ligands and central titanium (IV) ions, indicating framework incorporation of titanium in MCM-41. A band between 300 and 350 nm is absent, indicating that a (TiO_2) phase is not formed in these samples during crystallization or upon calcination. These results are consistent with previous work.[23]

Upon introduction of chromium into TiMCM-41, the maximum of the 265-nm band of TiMCM-41 shifts to 278 nm in Cr/TiMCM-41 (Figure 8). This reveals an interaction between the chromium species and titanium. Another broad band centered at 358 nm shows that dichromate dominates in Cr/TiMCM-41. Compared with Cr/AlMCM-41, there are no 446- and 600-nm bands in these spectra, which indicates that Cr_2O_3 clusters are not formed. The intensity of the band at 278 nm is much larger than that of the 358-nm band, which is due to the transition of O → Ti(IV). For 2% CrO_3/3% TiO_2/ SiO_2, in addition to the dichromate absorption, an absorption around 600 nm is visible. This indicates Cr_2O_3 formation on the TiO_2 surface.[19]

Framework Metal Ions. Figure 9 shows the UV−vis spectra of Cr/MCM-41 with different framework metal ions. For Cr/ZrMCM-41, in addition to the 275- and 350-nm absorptions,

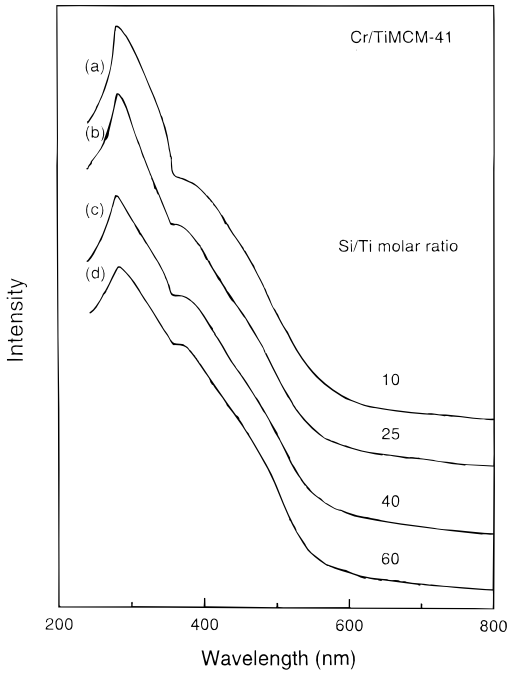

Figure 8. Diffuse reflectance UV−vis spectra of of Cr/TiMCM-41 with various Si/Ti ratios: (a) Si/Ti= 10, (b) Si/Ti = 25, (c) Si/Ti = 40, and (d) Si/Ti = 60.

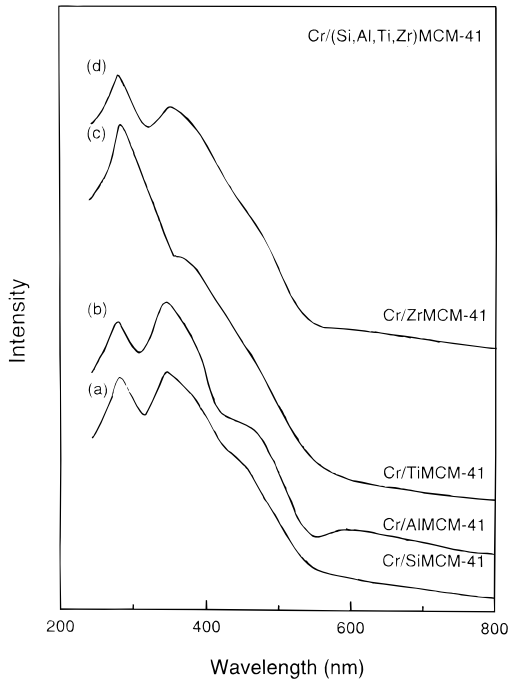

Figure 9. Diffuse reflectance UV−vis spectra of Cr/MeMCM-41 (Me = Al, Ti, and Zr) with Si/Me = 25 and Cr/SiMCM-41: (a) Cr/SiMCM-41, (b) Si/Al = 25, (c) Si/Ti = 25, and (d) Si/Zr = 25.

there are weak bands around 445 and 600 nm that indicate the presence of Cr_2O_3. The spectrum of Cr/SiMCM-41, which is similar to that of Cr/SiO_2, is also composed of four bands at 275, 350, 445, and 600 nm. This shows that dichromate and Cr_2O_3 coexist. In addition, the amount of Cr_2O_3 derived from the UV−vis spectra is in the order Cr/TiMCM-41 < Cr/ZrMCM-41 < Cr/SiMCM-41 < Cr/AlMCM-41. This is consistent with the ESR results.

TPR. *Framework Si/Al Ratio.* TPR has been largely used to study supported mono- and bimetallic catalysts. Metal oxides supported on Al_2O_3 or SiO_2 and unsupported oxides may exhibit

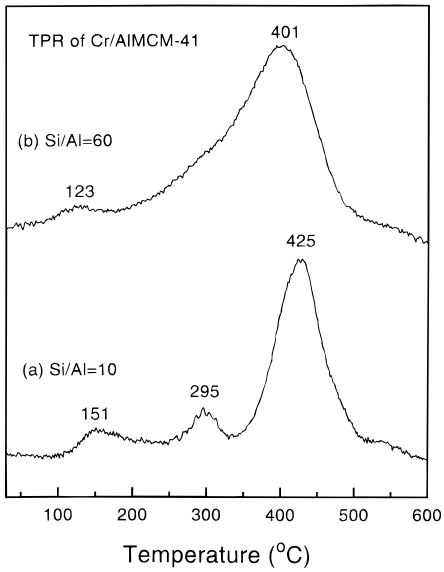

Figure 10. TPR profiles of Cr/AlMCM-41 with two Si/Al ratios: (a) Si/Al = 10 and (b) Si/Al = 60.

TABLE 2: Hydrogen TPR Data for Cr/MeMCM-41(Me = Al, Ti, and Zr) and Cr/SiMCM-41

samples	temperature of maximum H_2 consumption/°C	H_2 consumption (μmol/g sample)	average oxidation state
Cr/AlMCM-41 (Si/Al = 60)	401	338.9	4.76
Cr/AlMCM-41 (Si/Al = 10)	425	218.5	4.14
Cr/TiMCM-41 (Si/Ti = 60)	423	356.1	4.85
Cr/TiMCM-41 (Si/Ti = 10)	403	249.7	4.29
Cr/ZrMCM-41 (Si/Zr = 25)	413	247.6	4.29
Cr/SiMCM-41	430	339.2	4.76

different reduction behaviors. TPR of Cr/Al_2O_3, Cr/SiO_2, and Cr on alumina pillared clay has been studied.[6,7,20,24] Figure 10 shows the TPR profiles of Cr/AlMCM-41 with variable Si/Al ratios. The peak maximum shifts from 401 °C to 425 °C with an estimated accuracy of ±2 °C with increasing Al content. It is noteworthy that the reduction temperature is dependent on the reduction conditions, such as the H_2 partial pressure and the heating rate. It is therefore difficult to discuss the reduction temperature differences from the data obtained under different reduction conditions reported in the literature. The reported reduction temperatures are quite different, even for the same system in the literature. The width of the TPR peak around 400 °C broadens with decreasing aluminum content. Table 2 gives the amount of hydrogen consumed in the main peak (around 400 °C). The calculation of the average oxidation state in each sample is derived from the area under the TPR peak and from the amount of Cr, assuming that the reduction proceeds according to the stoichiometry $2CrO_3 + 3H_2 \rightarrow Cr_2O_3 + 3H_2O$. The calculated average oxidation states of Cr are summarized in Table 2, together with the temperature of maximum H_2 consumption. The H_2 consumption of Cr/AlMCM-41 decreased from Si/Al = 10 to Si/Al = 60. Accordingly, the average oxidation state of Cr in Cr/AlMCM-41 increases from Si/Al = 10 to 60. The results are slightly different from that of Cr/Al_2O_3·SiO_2. When supports with the same Cr loading are compared, the average oxidation state of Cr decreases from alumina to silica−alumina to silica.[20]

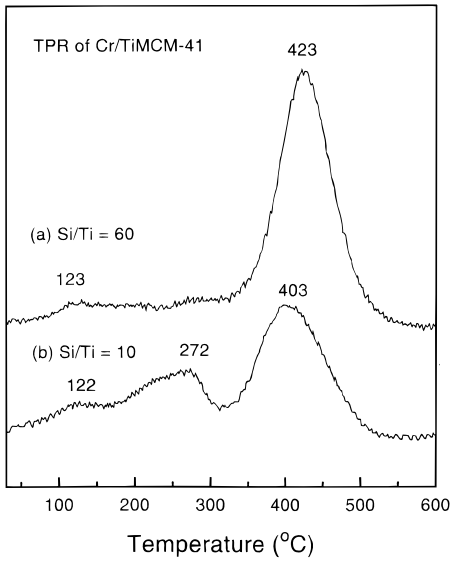

Figure 11. TPR profiles of Cr/TiMCM-41 with two Si/Ti ratios: (a) Si/Ti = 10 and (b) Si/Ti = 60.

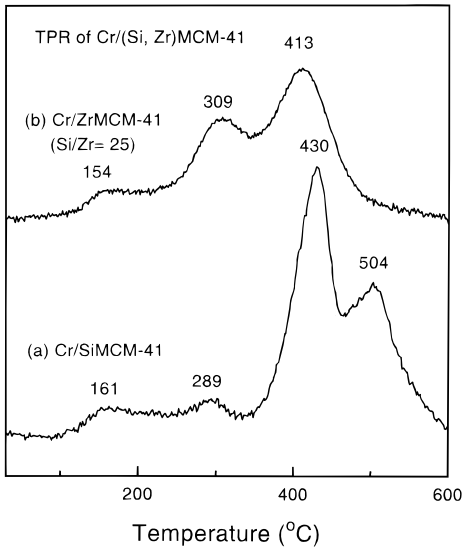

Figure 12. TPR profiles of (a) Cr/SiMCM-41 and (b) Cr/ZrMCM-41 with Si/Zr = 25.

Framework Si/Ti Ratio. The TPR profiles of Cr/TiMCM-41 with Si/Ti = 10 and 60 are shown in Figure 11. The maximum of the reduction peak shifts from 423 °C to 403 °C with increasing amount of Ti. The shifting trend is opposite to that of Cr/AlMCM-41. The H_2 consumption of the main peak (around 400 °C) decreases from 356.1 mmol/g sample to 249.7 mmol/g sample, and the average oxidation number decreases from 4.85 to 4.29, with an accuracy of ±0.01 with increasing Ti from Si/Ti = 60 to 10. The peak with a maximum at 272 °C is attributed to the reduction of Ti^{4+} to Ti^{3+}.

Framework Metal Ions. Figure 12 shows the TPR profiles of Cr/MCM-41 with different framework metal ions. The H_2 consumption and average oxidation number are shown in Table 2. Due to overlapping peaks, the areas are determined with 2% lower precision. The hydrogen consumption at 504 °C observed for Cr/SiMCM-41 could be due to reduction of Cr^{3+} to Cr^{2+}.

Raman Spectra. Figures 13 and 14 show Raman spectra of Cr/AlMCM-41 and Cr/TiMCM-41 with variable amounts of Al and Ti. The chromium loading on these samples is 2 wt %.

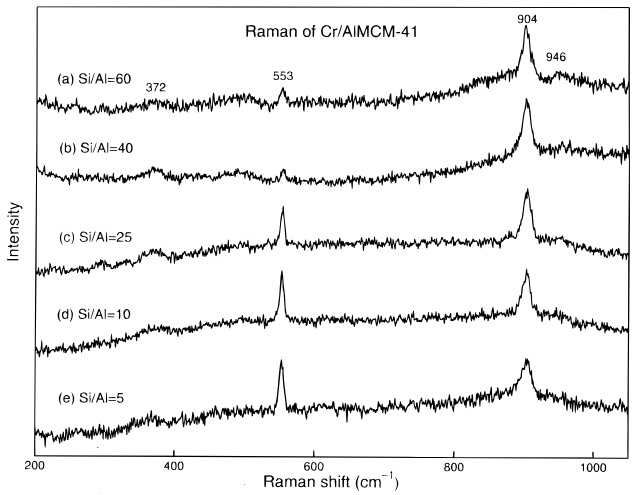

Figure 13. Raman spectra at 293 K of Cr/AlMCM-41 with various Si/Al ratios: (a) Si/Al = 60, (b) Si/Al = 40, (c) Si/Al = 25, and (d) Si/Al = 10, and (e) Si/Al = 5.

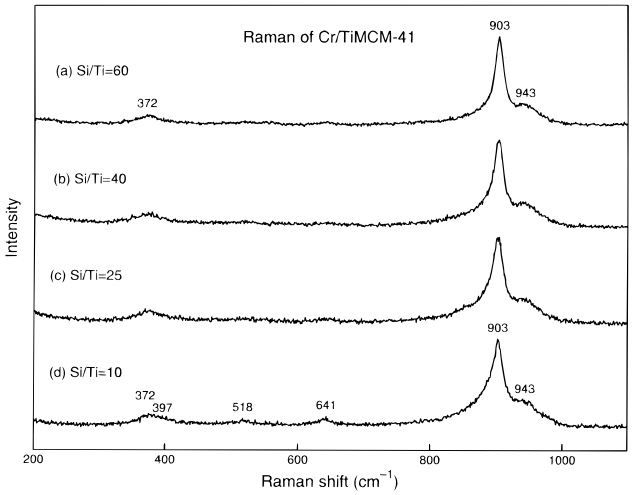

Figure 14. Raman spectra at 293 K of Cr/TiMCM-41 with various Si/Ti ratios: (a) Si/Ti = 60, (b) Si/Ti = 40, (c) Si/Ti = 25, and (d) Si/Ti = 10.

The Raman spectra of Cr/AlMCM-41 (Figure 13) exhibits bands at 372, 553, 904, and 946 cm^{-1}. The 372 cm^{-1} and 904 cm^{-1} bands are assigned to Cr−O bending and stretching modes, respectively, from hydrated dichromate ($Cr_2O_7^{2-}$).[1,25] The 553 cm^{-1} band is attributed to the Cr_2O_3 species.[26] As the amount of Al increases, the intensity of the 553 cm^{-1} band seems to increase, whereas that of the 904 cm^{-1} band seems to decrease. This suggests that the amount of Cr_2O_3 formed during calcination increases with the content of Al in Cr/AlMCM-41, whereas the amount of $Cr_2O_7^{2-}$ decreases, although it is difficult to quantitate Raman spectra.

In Figure 14, three bands at 372 cm^{-1}, 903 cm^{-1}, and 943 cm^{-1} (shoulder) indicate the existence of hydrated dichromate ($Cr_2O_7^{2-}$) in Cr/TiMCM-41with various amounts of Ti. The intensity of the 903 cm^{-1} band is almost the same for all the Cr/TiMCM-41 samples. For a Si/Ti ratio of 10, three additional bands are observed at 397 cm^{-1}, 518 cm^{-1}, and 641 cm^{-1} and are assigned to TiO_2 (anatase) particles.[27] In contrast to Cr/AlMCM-41, the 553 cm^{-1} band for Cr_2O_3 is not observed in all Cr/TiMCM-41 samples, perhaps with the exception of Cr/TiMCM-41 with a Si/Ti ratio of 60 (Figure 14a). This is consistent with the ESR spectra, in which a weak Cr_2O_3 signal in Cr/TiMCM-41 with Si/Ti > 25 is observed by ESR.

Discussion

Chemistry of Chromium in Cr/MeMCM-41 (Me = Al, Ti, and Zr) Materials and Comparison with $Cr/SiO_2 \cdot Al_2O_3$ and Cr/TiO_2. UV−vis, ESR, and Raman results for Cr/MeMCM-41 clearly show that Cr_2O_3 is present in SiMCM-41, ZrMCM-41, and AlMCM-41. With an increase of Al content in AlMCM-41, the amount of Cr_2O_3 also increases. However, Cr_2O_3 in Cr/TiMCM-41 was significantly reduced for Si/Ti < 25. The explanation could be as follows. During calcination, not only is physisorbed water removed, but also polychromate species are anchored to the MCM-41 surface by reaction with OH. This anchoring process can be envisaged as an acid−base reaction in which the weaker acid H_2O is replaced by the stronger acid H_2CrO_4. The most basic OH groups react preferentially, and the less basic OH groups only react at high Cr loadings. Silica surfaces contain more acid hydroxyl groups and, therefore, have poor capacity for Cr anchoring. Consequently, Cr_2O_3 particles are formed on SiMCM-41 even at low Cr loadings.

In $Cr/SiO_2 \cdot Al_2O_3$, the amount of Cr_2O_3 increases with the silica content.[20] There is an opposite trend for Cr/AlMCM-41. Surface hydroxyls on AlMCM-41 have been studied in detail.[10,28−31] The ^{29}Si MAS NMR spectra of AlMCM-41 and SiMCM-41 indicate that with a decrease of Si/Al the Q^3 peak intensity near −100 ppm due to $Si(OSi)_3OH$ sites increases.[10,28,29] Ammonia desorption investigations for AlMCM-41 with different Si/Al ratios confirm the presence of strong acid sites. The amount of desorbed NH_3 from these strong acid sites increases with increasing Al content in AlMCM-41.[30] The ion exchange levels also increase with increasing aluminum content in AlMCM-41.[31] These results suggest a higher number of strongly active sites present in AlMCM-41 compared with SiMCM-41. Since a more acidic hydroxyl group has a lower capacity for Cr anchoring, the amount of Cr_2O_3 increases with increasing aluminum content in AlMCM-41. This is confirmed by ESR, UV−vis, and Raman results for Cr/AlMCM-41. The average oxidation state of Cr/AlMCM-41 with Si/Al = 60 is larger than that of Cr/AlMCM-41 with Si/Al = 10. This indicates that the Cr_2O_3 amount in the former is larger than in the latter. These results also confirm that aluminum has been incorporated into the AlMCM-41 framework since if aluminum existed as Al_2O_3, the results observed for AlMCM-41 should be as for $Cr/SiO_2 \cdot Al_2O_3$.

Numerous studies have been published for TiMCM-41 with a focus on framework incorporation of Ti into MCM-41.[10,32−35] The IR spectrum of TiMCM-41 closely resembles that of SiMCM-41, and a band at 960 cm^{-1} is clearly visible in both TiMCM-41 and SiMCM-41. The strong intensity of this band in these samples is due to the large amount of silanol groups present in the calcined materials.[32] Ti incorporation into the framework of MCM-41 leads to an increase of cross-linking of the MCM-41 framework. This is evidenced by an increase in the fraction of Q^4 sites at the expense of both Q^2 and Q^3 framework sites observed by NMR.[34] A question is whether this decrease of OH concentration in TiMCM-41 compared to SiMCM-41 is large enough to account for the significant reduction of Cr_2O_3 in Cr/TiMCM-41 with Si/Ti < 25. The question of whether there is an interaction between Ti and Cr to stabilize Cr(VI) as Si−O−Ti−O−Cr(VI) was also raised in studies on $Cr/TiO_2/SiO_2$.[19,20]

Surface monochromate and polychromate species were observed on $TiO_2(3\%)/SiO_2$ which possesses an orange color and an additional UV−vis band around 454 nm. The corresponding CrO_3/SiO_2 material did not exihibit this additional band or an orange color. Therefore, polychromates are associated with surface titania sites. These observations are consistent with the chromate:polychromate ratios on TiO_2/SiO_2 and SiO_2, showing a higher amount of polychromate on TiO_2/SiO_2. Apparently, titania prefers to coordinate polychromates. A 3% CrO_3 in TiO_2/SiO_2 material atomic ratio of Cr:Ti ∼ 0.9 reflects the maximum amount of surface Cr and Ti oxides that can be dispersed as a two-dimensional overlayer on this silica. This suggests that on average one surface Cr atom is associated with one surface Ti atom. The interaction between surface chromate and a surface titania site is consistent with the low affinity of silica for metal oxides. There is no direct spectroscopic evidence for the coordination of surface monochromate to surface titania.[19]

The interaction between titanium and chromium in Cr/TiMCM-41 has been established based on the following. First, the maximum of the 265-nm band of TiMCM-41 shifts to 278 nm in Cr/TiMCM-41. Second, the TPR profile shows easier reduction of Cr(VI) in Cr/TiMCM-41 with Si/Ti = 10 compared with Cr(VI) in Cr/TiMCM-41 with Si/Ti = 60. Third, the Si−O−Cr linkage does not stabilize Cr as Cr(VI) in Cr/SiMCM-41, since Cr_2O_3 is detectable by UV-vis and ESR. By ESR, the Cr and Al interaction is apparent in Cr/AlMCM-41 by a line width increase. By ESEM, Al modulation clearly shows the affinity of Cr to Al for Cr/AlMCM-41.[36] These conclusions can be extended to Cr/TiMCM-41.

Molecular Structure of Cr(VI) in Cr/(Si, Al, Ti, and Zr)-MCM-41 and Comparison with Cr(VI) in Cr/oxides and CrMCM-41. Chromium oxides supported on inorganic oxides such as silica, alumina are catalysts for polymerization, dehydrogenation, oxidation, and isomerization reactions. The activity of Cr for such a wide spectrum of reactions is based on the variability of its oxidation states, coordination environment, and degrees of polymerization of chromium oxide species. The Philips Cr/silica polymerization catalyst is prepared by impregnation of a chromium compound onto a wide-pore silica followed by calcining in oxygen to activate the catalyst.[37] This leaves Cr(VI) species dispersed on the surface.

Chromium(VI) oxide compounds prefer tetrahedral coordination. Tetrahedrally coordinated chromium can be monochromate(CrO_4^{2-}), dichromate($Cr_2O_7^{2-}$), trichromate($Cr_3O_{10}^{3-}$), or tetrachromate ($Cr_4O_{13}^{2-}$), both in aqueous solution and in solids.[38] The molecular structure of surface chromium oxides is strongly dependent on the Cr loading, activation temperature, hydroxyl concentration, and surface area. Direct information about the molecular structure of Cr(VI) can be found by the application of diffuse reflectance UV−vis and Raman spectroscopies.

Under hydrated conditions, the dispersion of Cr(VI) depends on the isoelectric point of the amorphous oxide.[1] A lower isoelectric point results in a higher H^+ concentration near the surface and the formation of dichromate by $2CrO_4^{2-} + 2H^+ \rightarrow Cr_2O_7^{2-} + H_2O$. Spectroscopic measurements on supported Cr with low Cr loadings show that the monochromate:dichromate ratio decreases with increasing Si:Al ratio for silica aluminas and that monochromate is observed on ZrO_2 and TiO_2, but mainly dichromate is observed on SiO_2. The Raman and UV−vis spectra show that both polychromate and monochromate are present on a surface titania overlayer on SiO_2, whereas surface polychromate is present on TiO_2 as well as on a physical mixture of TiO_2 and SiO_2 because Cr(VI) preferentially coordinates to titania.[19]

UV−vis spectra of Cr/AlMCM-41 with variable Si/Al ratios are dominated by two intense O → Cr(VI) charge-transfer bands of dichromate around 280 and 350 nm. The Raman spectra of

Cr/AlMCM-41 (Figure 13) exhibits bands at 372, 553, and 904 cm^{-1}. The 372 cm^{-1} and 904 cm^{-1} bands are assigned to Cr−O bending and stretching modes, respectively, for hydrated dichromate ($Cr_2O_7^{2-}$). The broad UV−vis band centered at 358 nm shows that dichromate dominates in Cr/TiMCM-41. In Figure 14, three Raman bands at 372, 903, and 943 cm^{-1} (shoulder) indicate the presence of hydrated dichromate ($Cr_2O_7^{2-}$) in Cr/TiMCM-41 with various amounts of Ti.

In calcined CrMCM-41, a band around 440 nm characteristic of polychromate is absent in the UV−vis spectrum, and a Raman band at 986 cm^{-1} indicates that Cr(VI) is present as a monochromate species.[22] In addition, Cr_2O_3 was not detected in calcined CrMCM-41.[22] So, we can improve the degree of Cr dispersion in MCM-41 materials by adding both Ti and Cr to the synthesis gel to form Cr/TiMCM-41. The dispersion difference between Cr/MeMCM-41 and Cr/metal oxides might be attributed to surface acidity, which is greater for MeMCM-41 than for metal oxides.

Cr(III) and Cr(V) in Cr/Me(Me = Al, Ti, and Zr)MCM-41 and Comparison with CrMCM-41 and Cr/SiO_2, Al_2O_3, TiO_2, and ZrO_2. The structures of Cr(III) and Cr(V) species on various zeolites and other supports has been much stuided.[12−16] This is not as true for Cr/MeMCM-41 materials. The intensity of the ESR β-signal increases in the order ZrMCM-41 < SiMCM-41 < AlMCM-41. The line width of the β-signal remains the same, but its intensity increases with decreasing Si/Al ratio. This indicates that the amount of Cr_2O_3 increases when the framework aluminum content increases in AlMCM-41. For Cr/TiMCM-41, we observe the opposite trend. At a higher Si/Ti ratio, the β-signal is observed, whereas it is significantly reduced at Si/Ti = 25.

As-synthesized CrMCM-41 shows an ESR signal at $g = 2.05$, which was assigned to hydrated Cr(III) in the MCM-41 wall.[22] Cr/ZrO_2 shows a spectrum with $g = 1.98$ and $\Delta Hpp = 480-500$ G assigned to segregated Cr_2O_3 on the surface of ZrO_2.[15] The ESR spectra of Cr/TiO_2 consist of a broad line at $g = 1.98$ assigned to magnetically interacting Cr(III) surface ions.[14] On Cr/Al_2O_3, an ESR signal with $g = 2.45-2.09$ and $\Delta Hpp = 1200-2000$ G was assigned to Cr_2O_3 clusters.[13] The absence of an ESR β-signal on Cr/SiO_2 was attributed to line broadening beyond dectection.[13]

The surface chemistry of Cr(V) on amorphous supports is more diverse, and chromyl cations can have different coordination geometries depending on the support composition. Two main Cr(V) coordination environments with slightly different ESR parameters are observed. In Cr/Al_2O_3, the close proximity of Al is evident from broadening of the Cr(V) ESR lines on Al_2O_3 with respect to SiO_2, a difference in the g-factors of the Cr(III) ESR lines on Al_2O_3 with respect to SiO_2, and a decrease of the ^{27}Al NMR line intensity with Cr loadings.[13] It is also interesting that the ESR signals of Cr(V) on SiO_2/Al_2O_3 resemble those of Al_2O_3, suggesting that Cr(V) is preferentially located in the Al_2O_3.[12] In Cr/ZrO_2, a strong interaction with the support stablizes isolated Cr(V) ions and prevents extensive clustering of Cr(III) during reduction.[15] The amount of Cr(V) on ZrO_2 is higher than on SiO_2 or Al_2O_3. Studies of Cr/TiO_2 show quite different results. An earlier study showed that surface Cr(V) species on titania were not stable at calcination temperatures and appeared to be converted to a lower chromium oxidation state.[14] A later study suggests that Cr(V) ions are situated on the surface of Cr_2O_3 or at a Cr_2O_3/TiO_2 boundary.[14] More recently, surface chromium oxide species are associated with titania on silica.[19] The overall intensity of Cr(V) increases in the order AlMCM-41 < SiMCM-41 < TiMCM-41 < ZrMCM-41. The intensity of the ESR β-signal increases in the order TiMCM-41 < ZrMCM-41 < SiMCM-41 < AlMCM-41. These results show that Ti and Zr stabilize Cr(V) compared to Al and Si.

Conclusions

A combination of ESR, UV−vis and Raman spectroscopies, and TPR was used successfully to characterize the chemical environment of chromium in Cr/MeMCM-41 (Me = Al, Ti and Zr). UV−vis, ESR, and Raman show that Cr_2O_3 is present in SiMCM-41, ZrMCM-41, and AlMCM-41. With increasing Al content in AlMCM-41, the amount of Cr_2O_3 increases, which contrasts with Cr/SiO_2·Al_2O_3. Cr_2O_3 is significantly reduced in Cr/TiMCM-41 for Si/Ti < 25. The results indicate a strong interaction between chromium and surface titanium centers that immobilizes the chromium species and prevents the formation of Cr_2O_3. UV−vis and Raman spectra show that Cr/MeMCM-41 materials are dominated by dichromate. The overall intensity of Cr(V) increases in the order AlMCM-41 < SiMCM-41 < TiMCM-41 < ZrMCM-41. The intensity of the ESR β-signal increases in the order TiMCM-41 < ZrMCM-41 < SiMCM-41 < AlMCM-41. These results show that Ti and Zr stabilize Cr(V) and Cr(VI) compared to Al and Si in MCM-41.

Acknowledgment. This research was supported by the National Science Foundation and the Robert A. Welch Foundation. M.H. and L.K. thank the NSF and the Deutscher Akademischer Austauschdienst (DAAD) for travel grants.

References and Notes

(1) (a) Weckhuysen, B. M.; Wachs I. E.; Schoonheydt, R. A. *Chem. Rev.* **1996**, *96*, 3327. (b) Weckhuysen, B. M.; Schoonheydt, R. A. *Catal. Today* **1999**, *51*, 223. (c) Weckhuysen, B. M.; Schoonheydt, R. A. *Catal. Today* **1999**, *51*, 215.

(2) Pullukat, T. J.; Hoff, R. E.; Shida, M. *J. Polym. Sci. Polym. Chem. Ed.* **1980**, *18*, 2857.

(3) Conway, S. J.; Falconer, J. W.; Rochester, C. H. J. *Chem. Soc., Faraday Trans. 1* **1989**, *85*, 71.

(4) Conway, S. J.; Falconer, J. W.; Rochester, C. H.; Downs, G. W. *J. Chem. Soc., Faraday Trans. 1* **1989**, *85*, 1841.

(5) Daniel, M. P.; Welch, M. B.; Dreiling, M. J. *J. Catal.* **1983**, *82*, 118.

(6) Jozwiak, W. K.; Dalla Lana, I. G. *J. Chem. Soc., Faraday Trans.* **1997**, *93*, 2583.

(7) Grazybowska, B.; Sloczynski, J.; Grabowski, R.; Wcislo, K.; Kozlowsk, A.; Stoch, J.; Zielinski, J. *J. Catal.* **1998**, *178*, 687.

(8) (a) Weckhuysen, B. M.; Bensalem, A.; Schoonheydt, R. A. *J. Chem. Soc., Faraday Trans.* **1998**, *94*, 2011. (b) Ramachandra Rao, R.; Weckhuysen, B. M.; Schoonheydt, R. A. *J. Chem. Soc., Chem. Commun.* **1999**, 445.

(9) (a) Casci, J. L. In *Advanced Zeolite Science and Application Studies*; Jansen, J. C., Stocker, M., Karge, H. G., Weitkamp, J., Eds.; Elsevier: Amsterdam, 1994; pp 329−356. (b) Luan, Z.; He, H.; Zhou, W.; Cheng, C.; Klinowski, J. *J. Chem. Soc., Faraday Trans.* **1995**, *91*, 2955.

(10) Keijzers, C. P.; Reijerse, E. S.; Stam, P.; Dumont, M. F.; Gribnau, M. C.; *J. Chem. Soc., Faraday Trans. 1* **1987**, *83*, 3493.

(11) Czernuszewicz, R. S. In *Methods in Molecular Biology*; Jones, C., Mulloy, B., Thomas, A. H., Eds.; Humana Press: Totowa, NJ, 1993; Vol. 17, pp 345−374.

(12) Cordishi, D.; Campa, M. C.; Indovina, V.; Occhiuzzi, M. *J. Chem. Soc., Faraday Trans.* **1994**, *90*, 207.

(13) (a) Weckhuysen, B. M.; De Ridder, L. M.; Grobet, P. J.; Schoonheydt, R. A. *J. Phys. Chem. B* **1995**, *99*, 320. (b) Weckhuysen, B. M.; Schoonheydt, R. A.; Mabbs, F. E.; Collison, D. *J. Chem. Soc., Faraday Trans.* **1996**, *92*, 2431.

(14) Kohler, K.; Schlapfer, C. W.; Zelewsky, A. V.; Nickl, J.; Engweiler, J.; Baiker, A. *J. Catal.* **1993**, *143*, 201.

(15) Cimino, A.; Cordischi, D.; Rossi, S. D.; Ferraris, G.; Gazzoli, D.; Indovina, V.; Occhiuzzi, M.; Valigi, M. *J. Catal.* **1991**, *127*, 761.

(16) Cordischi, D.; Indovina, V.; Occhiuzzi, M. *J. Chem. Soc., Faraday Trans.* **1991**, *87*, 3443.

(17) Weckhuysen, B. M.; Verberckmoes, A. A.; De Baets, A. R.; Schoonheydt, R. A. *J. Catal.* **1997**, *166*, 160.

(18) Weckhuysen, B. M.; Verberckmoes, A. A.; Buttiens, A. L.; Schoonheydt, R. A. *J. Phys. Chem.* **1994**, *98*, 579.

(19) Jehng, J.; Wachs, I. E.; Weckhuysen, B. M.; Schoonheydt, R. A. *J. Chem. Soc., Faraday Trans.* **1995**, *91*, 953.
(20) Weckhuysen, B. M.; Jehng, J.; Wachs, I. E.; Schoonheydt, R. A.; Cho, S. J.; Ryoo, R.; Kijlstra, S.; Poels, E. *J. Chem. Soc., Faraday Trans.* **1995**, *91*, 3245.
(21) Weckhuysen, B. M.; De Ridder, L. M.; Schoonheydt, R. A. *J. Phys. Chem.* **1993**, *97*, 4756.
(22) Zhu, Z.; Chang, Z.; Kevan, L. *J. Phys. Chem. B* **1999**, *103*, 2680.
(23) Luan, Z.; Kevan, L. *J. Phys. Chem. B* **1997**, *101*, 2020.
(24) Storaro, L.; Ganzerla, R.; Lenarda, M.; Zanoni, R.; Lopez, A. J.; Olivera-Pastor, P.; Castellon, E. R. *J. Mol. Catal. A, Chemical* **1997**, *115*, 329.
(25) (a) Michel, G.; Cahoy, R. *J. Raman Spectrosc.* **1986**, *17*, 4. (b) Michel, G.; Machiroux, R. *J. Raman Spectrosc.* **1983**, *14*, 22.
(26) Hardcastle, F. D.; Wachs, I. E. *J. Mol. Catal.* **1988**, *46*, 173.
(27) Went, G. T.; Oyama, S. T.; Bell, A. T. *J. Phys. Chem.* **1990**, *94*, 4240.
(28) Luan, Z.; Cheng, C.; Zhou, W.; Klinowski, J. *J. Phys. Chem.* **1995**, *99*, 1018.
(29) Zhao, X. S.; Lu, G. Q.; Whittaker, A. K.; Millar, G. J.; Zhu, H. Y. *J. Phys. Chem.* **1997**, *101*, 6525.
(30) Reddy, K. R.; Araki, N.; Niwa, M. *Chem. Lett.* **1997**, *7*, 637.
(31) Kim, J. M.; Kwak, J. H.; Jun, S.; Ryoo, R. *J. Phys. Chem.* **1995**, *99*, 16742.
(32) Blasco, T.; Corma, A.; Navarro, M. T.; Pariente, J. P. *J. Catal.* **1995**, *156*, 65.
(33) Alba, M. D.; Luan, Z.; Klinowski, J. *J. Phys. Chem.* **1996**, *100*, 2178.
(34) Zhang, W.; Froba, M.; Wang, J.; Tanev, P. T.; Wong, J.; Pinnavaia, T. J. *J. Am. Chem. Soc.* **1996**, *118*, 9164.
(35) Prakash, A. M.; Sung-Suh, H. M.; Kevan, L. *J. Phys. Chem. B.* **1998**, *102*, 857.
(36) Luca, V.; MacLachlan, D. J.; Bramley, R.; Morgan, K. *J. Phys. Chem.* **1996**, *100*, 1793.
(37) (a) McDaniel, M. *Adv. Catal.* **1985**, *33*, 47. (b) McDaniel, M. *Ind. Eng. Chem. Res.* **1988**, *27*, 1559.
(38) Vuurman, M.; Wachs, I. E. *J. Phys. Chem.* **1992**, *96*, 5008.